Macromolecules

Article

pubs.acs.org/Macromolecules

Solid-state Studies of the Crystalline/Amorphous Character in Linear *Poly*(ethylenimine hydrochloride) (PEI·HCl) Polymers and Their Copper Complexes

Juan Manuel Lázaro-Martínez,*[,†,∥] Enrique Rodríguez-Castellón,[‡] Daniel Vega,[§,#] Gustavo Alberto Monti,[⊥] and Ana Karina Chattah[⊥]

[†]CONICET, Av. Rivadavia 1917 (C1033AAJ), CABA, Argentina

[∥] Departamento de Química Orgánica, Facultad de Farmacia y Bioquímica, Universidad de Buenos Aires, Junín 956 (C1113AAD), CABA, Argentina

[‡]Departamento de Química Inorgánica, Cristalografía y Mineralogía, Facultad de Ciencias, Universidad de Málaga, Campus de Teatinos, Málaga, 29071, Spain

[§]Departamento de Física de la Materia Condensada, Comisión Nacional de Energía Atómica, Av. Gral. Paz 1499, 1650 San Martín, Buenos Aires, Argentina

[#]Escuela de Ciencia y Tecnología, Universidad Nacional de General San Martín, Buenos Aires, Argentina

[⊥]FaMAF-Universidad Nacional de Córdoba and IFEG-CONICET, Medina Allende s/n (X5000HUA), Córdoba, Argentina

Supporting Information

ABSTRACT: Linear poly(ethylenimine hydrochloride) (PEI·HCl) polymers with different molecular weights (22, 87, and 217 kDa) and their copper complexes (Cu–PEI) were studied with particular attention to the crystalline/amorphous character of the polymeric chains in lyophilized and crystallized samples by using 1D and 2D *solid-state* nuclear magnetic resonance, X-ray photoelectron spectroscopy, and X-ray diffraction techniques. Different $^{13}C\{^{1}H\}$ cross-polarization and magic angle spinning experiments using delayed contact time, ^{1}H dipolar filter and ^{1}H spin-lock filter were crucial to determine the different mobility domains in the crystallized and lyophilized samples of PEI·HCl and Cu–PEI. ^{13}C direct polarization experiments allowed the quantification of the crystalline/amorphous segments in each sample. The lyophilization process produced an increase in the amorphous fraction, even when some ordered domains were present, whereas the coordination of copper/sulfate ions produced a significant decrease in the mobility of polymer chains, leading to homogeneous and ordered materials even when Cu was desorbed.

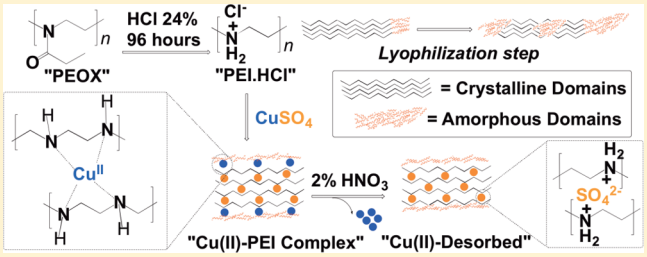

1. INTRODUCTION

The linear poly(ethylenimine) (PEI) polymer has many applications.[1−3] It has been used as a cosmetic ingredient to adjust viscosity, as a chelating metal ion to inhibit corrosion, and as a copolymer to develop energy storage devices.[4−7] In addition, PEI is a strong inhibitor of human papillomavirus and cytomegalovirus infections.[8] Interestingly, due to its biocompatibility, PEI has been used in biotechnology as nonviral vector to carry out gene transfection processes.[9,10] In particular, the transfer of genes to mammalian cells represents the basis for a technology platform of importance in animal production. The best-known transfection agents are viral, but their use can generate genetic disorders in the host cells. Therefore, the development of new soluble polymeric systems to perform efficient transfection processes is interesting as these polymers represent alternatives to the transfection reagents commonly used.[4,11−16] Cationic polymers bind DNA through electrostatic interactions, are nonviral gene delivery vehicles and are widely used.[11,17] Many factors, such as the molecular weight, surface charge, charge density, and hydrophilicity, affect the transfection efficiency of these polymers.[18] Therefore, it is necessary to optimize and develop new agents to achieve high transfection efficiency in the process.

Because of the importance of PEI polymers, their characterization in the solid state by powder X-ray diffraction,[19−22] infrared,[23,24] Raman[25] and thermal studies,[26] among others,[1,27,28] has received special attention. In particular, the hygroscopic behavior of nonprotonated PEI ($PEI_{free\text{-}base}$) samples has been directly related to the formation of different crystalline hydrates, as reported by Chatani et al. from X-ray studies.[19,20] Depending on the stoichiometric amounts of water present in the crystal lattice, crystals can be in the anhydrate,

Received: November 14, 2014
Revised: January 22, 2015
Published: January 30, 2015

DOI: 10.1021/ma5023082
Macromolecules 2015, 48, 1115−1125

Scheme 1. Synthesis of PEI Samples

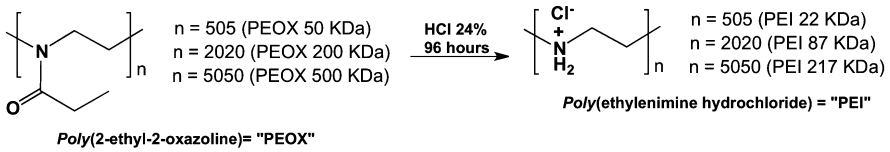

hemihydrate, sesquihydrate or dihydrate state, containing 0, 0.5, 1.5, or 2 water molecules per monomeric unit of $PEI_{free\text{-}base}$ ($-CH_2CH_2NH-$), respectively. In the anhydrate state, the $PEI_{free\text{-}base}$ chains exist as double-stranded helices, distinct from the fully extended planar-zigzag conformation in the sesquihydrate and dihydrate states due to the intermolecular hydrogen bonds with water molecules.[19−21,26] Among the information available for $PEI_{free\text{-}base}$, we found no information regarding PEI·HCl samples in the solid state, which is the chemical form used for transfection processes.[29] In addition, this polyelectrolyte material is lyophilized and can be stored at room temperature for extended periods without losing activity and reconstituted in a reproducible manner immediately before use.[30,31] For that reason, in the present study, we analyzed the impact of the lyophilization process in PEI·HCl samples in the solid state. The main aim was to study the structural and dynamic homogeneity of three synthetic variants of linear PEI·HCl with different molecular weights (22, 87, and 217 kDa) in the crystallized or lyophilized states through 1D and 2D *solid-state* nuclear magnetic resonance (*ss*-NMR) spectroscopy, together with X-ray photoelectron spectroscopy (XPS) and X-ray powder diffraction (XRPD) measurements. In addition, changes after the uptake of Cu(II) ion by these polymeric matrices were explored, given the importance in the removal of heavy metal ions[32−35] and the activation of hydrogen peroxide by the heterogeneous catalysts of Cu(II) for the degradation of pollutants with high environmental impact.[36−38]

2. EXPERIMENTAL SECTION

2.1. Synthesis of PEI·HCl. Linear poly(ethylenimine hydrochloride) (PEI·HCl) polymers, from now on called PEI, with molecular weights of 22, 87, and 217 kDa were synthesized from the corresponding poly(2-ethyl-2-oxazoline) from Sigma-Aldrich of 50, 200, and 500 kDa, respectively (Scheme 1). General procedure: 1 g of poly(2-ethyl-2-oxazoline) was added to 120 mL of a 24% HCl solution and refluxed for 96 h. The poly(2-ethyl-2-oxazoline) became dissolved in about 1 h. Two hours later, a white solid material (PEI) appeared in the flask and persisted throughout the rest of the reaction. Then, the reaction mixture was filtered and the white solid was washed with 5 mL of Milli-Q water. After that, the solid was air-dried for 48 h (this solid is called "crystallized PEI sample"). In addition, the crystallized solid was dissolved in Milli-Q water and the corresponding PEI solution was lyophilized overnight (this solid is called "lyophilized PEI sample"). The product was identified and its quality analyzed by ^1H and ^{13}C NMR spectroscopy. ^1H NMR (D_2O, 500 MHz) δ (ppm): 3.58 (s) and ^{13}C NMR (D_2O, 125 MHz) δ (ppm): 42.7.

2.2. Preparation of the Copper Complexes and Copper-Desorbed Polymers. The copper complexes were prepared from 150 mg of the crystallized PEI samples dissolved in 2 mL Milli-Q water. Then, 3 mL of a 0.1 M of copper(II) sulfate ($CuSO_4$) solution were added slowly and the corresponding Cu(II) complexes started to appeared. The solids were filtered, washed twice with 3 mL of water and dried at 60 °C for 24 h. The dried copper complexes were placed in a desiccator for 48 h prior to all measurements. The amount of Cu in the different Cu(II)−PEI complexes was around 30−40 mg per gram of material (3−4 wt %), as determined from the direct measurement of the solids through X-ray fluorescence (XRF) in an Advant XP^+ Thermo Electron spectrometer and from the acidic digestion of the solids in a Multiwave 3000 Anton Paar digestor and measured through high resolution inductively coupled plasma−mass spectrometry (HR−ICP−MS) in an Element XR Thermo spectrometer (Table S1, Supporting Information).

For the preparation of the Cu(II)-desorbed PEI polymers, 100 mg of Cu(II)−PEI complexes was dispersed in 10 mL of 2% of HNO_3 solution for 1 h. Then, the solids were filtered, washed twice with 10 mL of water and dried at 60 °C for 24 h. The dried Cu(II)-desorbed PEI polymers were placed in a desiccator for 48 h prior to all measurements. To ensure the complete removal of Cu ions, the solids were analyzed as in the Cu(II) complexes, corroborating the absence of Cu in the samples.

2.3. X-ray Photoelectron Spectroscopy. X-ray photoelectron spectra were collected using a Physical Electronics PHI 5700 spectrometer with non monochromatic Mg Kα radiation (300 W, 15 kV, 1253.6 eV) for the analysis of the core level signals of C 1s, N 1s, O 1s, S 2p, Cl 2p, and Cu 2p and with a multichannel detector. The used sensitivity factors for the studied elements were C 1s (0.314), N 1s (0.499), O 1s (0.733), S 2p (0.717), Cl 2p (0.954), and Cu 2p (4.395). The PHI ACCESS ESCA-V6.0 F software package was used for acquisition and data analysis. A Shirley-type background was subtracted from the signals. Recorded spectra were always fitted using Gaussian−Lorentzian curves, in order to determine the binding energy of the different element core levels more accurately. The error in BE was estimated to be *ca.* 0.1 eV. Powdered samples were pressed in a sample holder and then introduced in the preparation chamber and evacuated during one night at 10^{-7} Pa. Spectra of powdered samples were recorded with the constant pass energy values at 29.35 eV, using a 720 μm diameter analysis area. During data processing of the XPS spectra, binding energy values were referenced to the C 1s peak (284.8 eV) from the adventitious contamination layer. A short acquisition time of 10 min was used to examine C 1s, Cu 2p, and Cu LMM XPS regions in order to avoid, as much as possible, photoreduction of Cu^{2+} species. Nevertheless, a Cu^{2+} reduction in high vacuum during the analysis cannot be excluded.[39]

2.4. X-ray Powder Diffraction. X-ray powder diffraction (XRPD) patterns were recorded on an Empyrean diffractometer (Panalytical, The Netherlands), with a PixCel3D area detector in a 1D scanning lineal mode, over the 2θ range of 5−40°, using Cu Kα radiation (1.54184 Å) obtained from an X-ray generator set at 40 kV and 40 mA. Suitable samples for XRPD measurement were prepared in aluminum sample holders, at room temperature. Measurements were performed using a 0.5° divergence slit and 8 mm receiving slit, scanning step 0.0263°, counting time 200 s.

2.5. Solid-State NMR Experiments. High-resolution ^{13}C solid-state spectra for the polymers were recorded using the ramp $^1H-^{13}C$ CP-MAS sequence (cross-polarization and magic angle spinning) with proton decoupling during acquisition. All the solid-state NMR experiments were performed at room temperature in a Bruker Avance II-300 spectrometer equipped with a 4 mm MAS probe. The operating frequency for protons, carbons and nitrogens was 300.13, 75.46, and 30.42 MHz, respectively. Ammonium chloride was used as an external reference for the ^{15}N spectra and glycine was used as an external reference for the ^{13}C spectra and to set the Hartmann−Hahn matching condition in the cross-polarization experiments in both ^{15}N and ^{13}C spectra. The recycling time was 4 s. Different contact times during CP were employed in the range of 200−1500 μs for ^{13}C spectra. For ^{15}N spectra, a contact time of 3 ms and 800 μs were used for the PEI and Cu(II)−PEI samples, respectively. The SPINAL64 sequence (small phase incremental alternation with 64 steps) was used for heteronuclear decoupling during acquisition with a proton field H_{1H}

DOI: 10.1021/ma5023082
Macromolecules 2015, 48, 1115−1125

Table 1. Atomic Composition and Elemental Analysis (wt % in Parentheses) for the Indicated Samples Determined from XPS Measurements with the Amount of Water Estimated from Thermogravimetry Methods

material	C	N	Cl	O	Cu	S	H_2O (wt %)
crystallized PEI 87 kDa	61.02 (45.0)	19.32 (16.61)	15.96 (34.74)	3.71 (3.64)	–	–	9–11
lyophilized PEI 87 kDa	65.38 (50.19)	17.04 (15.25)	13.35 (30.25)	4.22 (4.31)	–	–	12–13
Cu(II)–PEI 87 kDa complex	46.28 (35.44)	15.94 (14.23)	0.69 (1.56)	28.10 (28.66)	0.87 (3.52)	8.11 (16.58)	10–12
Cu(II)-desorbed PEI 87 kDa	47.88 (38.40)	16.81 (15.71)	<0.01 (<0.02)	27.72 (29.60)	<0.01 (<0.04)	7.58 (16.23)	8–10

satisfying $\omega_{1H}/2\pi = \gamma_H H_{1H} = 62$ kHz.[40] ^{13}C natural abundance direct polarization experiments with proton decoupling (SPINAL64) during acquisitions were conducted for all the samples. An excitation pulse of 4.0 μs and a recycling time of 100 s was used and 400 scans were accumulated in order to obtain quantitative and good signal-to-noise ratio. The spinning rate for all the samples was 10 kHz.

The proton spin–lattice relaxation time in the rotating frame ($T_1\rho^H$) was measured via CP-MAS carbon spectra for the polymers and their copper-complexes. To measure $T_1\rho^H$ proton spin-lock field at $\omega_{1H}/2\pi = 40$ kHz was inserted as a function of a variable time τ, before the contact time step. The time τ was varied from 10 μs to 6 ms. The contact time was 100 μs, short enough to avoid spin diffusion between protons. The spinning rate for all the samples was 10 kHz. The proton spin–spin relaxation times (T_2^H) for the different samples were measured directly in the proton signal in static conditions with the Hahn-Echo experiment ($(\pi/2)|_x - \tau - \pi|_y - \tau$). The $\pi/2$ pulse was 4 μs and the variable time τ was varied from 5 to 600 μs.

Delayed ^{13}C CP was used to select the amorphous regions. In these experiments a τ_d time between the initial $\pi/2$ pulse on protons and the cross-polarization period is added (τ_d: 0–15 μs). In the dipolar filter (DF) selective pulse experiments, 12 pulses of 10 μs with a pulse spacing of 20 μs was used in order to enhance the signal from the amorphous fractions. For the spin-lock (SL) selective pulse sequence, the spin-lock time and the radio frequency amplitude were 5 ms and 60 kHz, respectively, giving rise only the signal from the crystalline regions.[41−43]

The 2D $^1H-^{13}C$ wideline separation experiment (2D WISE) was performed following the pulse sequence developed by Schmidt-Rohr et al.[44] The proton magnetization was transferred to ^{13}C using a short contact time of 200 μs to avoid equilibration of the proton magnetization due to spin diffusion. The MAS rate was set to 4.5 kHz in order not to affect the proton line shape. In our experiment, 32 increments of 3 μs were collected in the indirect ^1H dimension.

The 2D $^1H-^{13}C$ HETCOR experiments in the solid state were recorded following the sequence presented by van Rossum et al.[45] The contact time for the CP was 150 μs to avoid relayed homonuclear spin-diffusion-type processes. The magic angle pulse length was 2.55 μs. To obtain the ^1H spectra, 64 points were collected with a dwell time of 35.5 μs. The acquisition time was 1.14 ms and the spinning rate was 10 kHz.

3. RESULTS

3.1. XPS Analysis. First, XPS analysis of the polymer was conducted to determine the chemical composition in the samples after the different treatments performed (Figures S1 and S2, Supporting Information). The results, together with the amount of water estimated from the thermogravimetry results, are summarized in Table 1. The N 1s spectrum for the crystallized PEI samples was fitted using two Gaussian–Lorentzian peaks with binding energies of 399.0 (25%) and 401.0 eV (75%) interpreted as the nonprotonated and protonated nitrogens, respectively (Figure S3, Supporting Information). A 75% degree of protonation explained the high amount of chloride retained in the crystallized PEI samples, with a chloride as a counterion of the positive nitrogen. The water molecules in the different PEI samples may be randomly dispersed in the polymeric structure since the total amount of water estimated from the thermogravimetry results was 9–11% and a low content of oxygen was observed by XPS (Table 1). The N 1s spectrum of the lyophilized sample also showed two contributions at the same binding energy values as that of crystallized PEI but with a slight decrease in the protonation degree (from 75 to 70%) together with an increase in the oxygen content (Table 1 and Figure S3, Supporting Information).

The colorless PEI aqueous solutions showed no absorption bands in the UV–vis region, whereas their Cu complexes exhibited an intense blue-green color with an absorption band at 626 nm after the addition of a $CuSO_4$ solution, meanwhile the nonsoluble Cu(II) complexes of PEI started to appear. The shift of the absorption band from 789 nm in the $CuSO_4$ solution to 626 nm in the Cu(II)–PEI complexes confirmed the formation of $[CH_2-CH_2NH]_n$---Cu^{2+} complexes due to the bonding σ(N) → antibonding $d_{x^2-y^2}$(Cu) charge transfer. With the aim to study the coordination modes in this Cu(II) complex, we performed electron paramagnetic resonance (EPR) studies, but could not resolve the hyperfine structures in the parallel region. These results indicate that more than one coordination mode could be coexisting together with some Cu–Cu dipolar interaction or exchange coupling as a result of the short distance (<10–15 Å) between the Cu centers. The N 1s core level spectrum showed a similar shape but the two contributions were slightly shifted to higher binding energy values at 399.4 eV (28%) and 401.3 eV (72%) (Figure S3, Supporting Information). In addition, the Auger line for Cu (CuLMM) and the Cu 2p spectrum indicate that copper ions exist as Cu(I) species on the surface, according with the values of CuLMM kinetic energy of 914.3 eV and Cu $2p_{3/2}$ values at 932.7 eV (Figures S4 and S5, Supporting Information).[36] The fact that copper ions are in the form of Cu(I) on the surface was due to the reduction induced at ultrahigh vacuum applied for the acquisition of the XPS spectra (10^{-7} Pa).[39] Another contribution that facilitated this reduction was the low content in Cu in the bulk material (~3–4 wt % from the results of XRF and XPS results, Table S1, Supporting Information). In addition, no changes were observed in the N 1s spectrum to explain a possible oxidation of the nitrogen atoms and the concomitant reduction of Cu(II) species to Cu(I) during the coordination process (Figure S3, Supporting Information). Then, comparison of the Cu 2p spectra at short and long irradiation times for the Cu–PEI complex showed that at long irradiation times the contribution of satellite peaks was strongly affected by the photoreduction phenomenon of the residual Cu(II) on the surface, whereas at short irradiation times the reduction can only be interpreted from the effect at ultrahigh vacuum since the intensity ratio of the shakeup satellite and the intensity of the Cu $2p_{3/2}$ peak ($I_{Cu_{sat}}/I_{Cu_{2p}}$) was 0.17, which is far from the value found for Cu(II) species (CuO = 0.55) (Figure S5, Supporting Information).[46] Furthermore, the EPR spectrum clearly shows signals attributed to Cu(II) ions, since Cu(I) ions are not paramagnetic.

DOI: 10.1021/ma5023082
Macromolecules 2015, 48, 1115–1125

Additionally, the amount of oxygen in the Cu complexes increased as oxygen comes from the contribution of sulfate ions used in the preparation of the Cu complexes (S $2p_{3/2}$ energy of 167.8 eV). Also, the content of Cu determined from desorption experiments was of around 36 mg of Cu per gram of PEI 87KDa, which is in agreement with the XPS results. During the uptake of Cu^{2+} ions, the protons of the nitrogen ($-CH_2N\mathbf{H}_2^+CH_2-$) were released to coordinate the metal ion at the same time as chloride ions were exchanged by sulfate ions due to the important decrease in the Cl content and the Cu:S ratio (Table 1). The N 1s spectrum of the Cu(II)−PEI complex was similar to that of the crystallized PEI sample, indicating that the protonated or coordinated nitrogen atoms have a similar decrease in electron density (Figure S3, Supporting Information). Here, the amount of nitrogen coordinated with Cu^{2+} or protonated (with SO_4^{2-} or Cl^- as a counterion) is 72% and the rest of the neutral nitrogen is 28%, obtained from the fitting results.

Finally, when the Cu ions were desorbed from the Cu(II)−PEI complexes, the sulfate ions still remained in the polymer structure at the same time as the chloride ions were completely desorbed (Table 1). It is interesting to remark that the Cu(II)-desorbed PEI samples remained nonsoluble in aqueous media like the Cu(II)-complexes. For that reason the presence of sulfate in the samples (15 wt % sulfur (S) and 45 wt % SO_4^{2-}, Table S1, Supporting Information) was responsible for their solubility properties, since the PEI·HCl samples are completely soluble in water. Also, the N 1s spectrum did not change in the Cu(II)-desorbed samples in comparison with the Cu(II)−PEI complexes (Figure S3, Supporting Information).

3.2. XRPD Studies. Figure 1 displays the XRPD spectra corresponding to the crystallized and lyophilized PEI of 87 kDa.

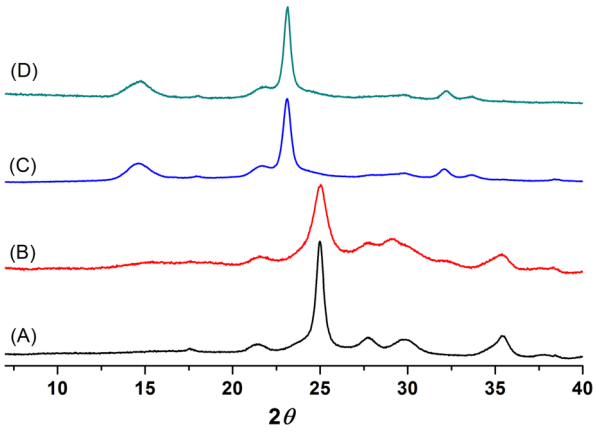

Figure 1. X-ray powder diffraction spectra for the crystallized (A), lyophilized (B), Cu(II) complex (C), and Cu(II)-desorbed samples of PEI 87 kDa (D).

In the following, only the behavior of the PEI 87 kDa sample is shown, being representative of the PEI samples of 22 and 217 kDa.

Figure 1 shows that the XRPD spectra were similar for the crystallized and the lyophilized PEI, indicating that the same "crystalline arrangement" was present regardless of the treatment of the polymers. In addition, the relative higher background signal of the XRPD pattern for the lyophilized sample in comparison with the crystallized one is indicative that an amorphous fraction was enhanced during the lyophilization step.

It is possible that the linear PEI chains in the crystal lattice may be stabilized through chloride anion and hydrogen bonding in the monomeric unit ($([CH_2CH_2NH_2^+\text{--}Cl^-]_n$-$[^+NH_2CH_2CH_2]_n$ or $\text{--}[NHCH_2CH_2]_n$) according with the XPS results and the previous results of Chatani et al. in sesquihydrate $PEI_{free\text{-}base}$ materials, where the polymer chains adopt the planar zigzag conformation.[19] In the systems reported here, the water molecules were randomly dispersed in the polymeric structure related to the monomeric unit, without relative importance in the stabilization of the crystal lattice[19,20,47] as in the hydrate samples in $PEI_{free\text{-}base}$ based on the lower content of water and oxygen obtained from the TG and XPS results, respectively. However, some other crystalline arrangements cannot be excluded, since it is difficult to determine the exact composition without an adequate crystalline sample.

The XRPD characterization of the Cu(II) complexes of the PEI polymers showed that they exhibit a XRPD profile completely different from that of the noncoordinated PEI samples. When Cu ions are coordinated through the nitrogen atoms of the PEI polymer, protons are exchanged by Cu^{2+} ions, giving rise to a different crystalline pattern with lower 2θ reflections in comparison with the corresponding nondoped polymers. Note that the main reflection in the Cu complex of PEI 87 kDa can be found at 23.1° while in the noncoordinated PEI samples it can be observed at 2θ of 25.0°. This difference may indicate an increase in the crystalline interplanar spacing from 3.564 Å in the noncoordinated PEI 87 kDa samples to 3.875 Å in the Cu complex ones. Also, a new diffraction peak appeared at 2θ of 14.5° with an interplanar spacing of 6.05 Å. The conformation of the unit cell changed after the coordination of Cu and sulfate ions since the interplanar distances increased upon the uptake of both Cu and SO_4^{2-} ions, which need greater volumes than the interactions between the polymer chains. However, the XRPD spectra of both the Cu(II)-desorbed PEI and Cu(II)−PEI samples were identical, indicating that the SO_4^{2-} ions produced a new organization of the polymer segments that remained unaltered after the desorption of Cu. If the Cu ions were substantially important in the crystalline domains, after their desorption from the Cu(II) complexes a new XRPD would be obtained.

3.3. ^{13}C and ^{15}N CP-MAS Experiments. The ^{13}C NMR solution spectra in D_2O recorded for both crystalline and lyophilized PEI 87 kDa samples resulted in a simple spectrum with a ^{13}C resonance at 43.5 ppm, indicating that all the methylene carbons ($-CH_2-$) were identical. The ^{13}C CP-MAS spectra for a lyophilized and a crystallized sample of PEI 87 kDa in comparison with their ^{13}C NMR spectrum in deuterium oxide solution are shown in Figure 2A. The ^{13}C CP-MAS spectrum for the crystallized sample shows a main carbon resonance signal at 42.9 ppm and a slight shoulder at 44.5 ppm, whereas the spectrum for the lyophilized sample displays two resolved signals at 42.9 and 44.5 ppm. These results indicate that during the synthetic process, most of the polymer chains crystallized adopting a regular and periodic conformation, as it can be seen from the XRPD results (Figure 1), giving rise to a sample with at least one predominant ordered component with a chemical shift at 42.9 ppm. However, if the crystallized sample is dissolved in Milli-Q water, the PEI chains adopt a random distribution, which is average in solution, giving an isotropic chemical shift at 43.5 ppm. Then, when this aqueous PEI solution was lyophilized, the ^{13}C CP-MAS presented two clearly resolved resonance signals at 42.9 and 44.5 ppm (Figure

DOI: 10.1021/ma5023082
Macromolecules 2015, 48, 1115−1125

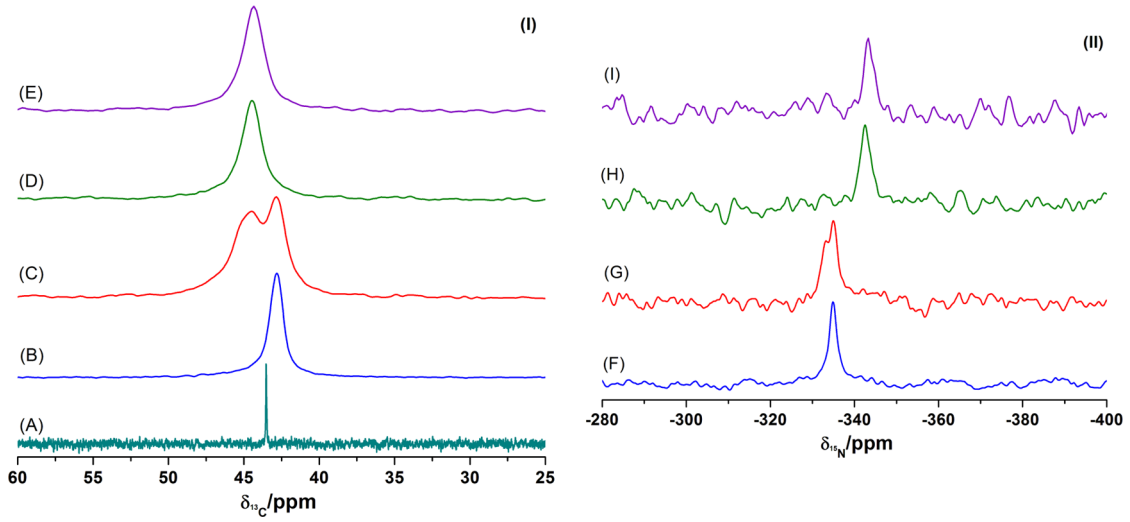

Figure 2. ^{13}C NMR spectra (**I**) for the PEI 87 kDa in deuterium oxide solution (A) and ^{13}C CP-MAS spectra for crystallized (B), lyophilized (C), Cu(II) complex (D), and Cu(II)-desorbed (E) samples of PEI 87 kDa. ^{15}N CP-MAS spectra (**II**) for crystallized (F), lyophilized (G), Cu(II) complex (H), and Cu(II)-desorbed (I) samples of PEI 87 kDa.

2), corresponding to the crystalline and amorphous regions, respectively, as shown in the following sections. In the lyophilization process, the polymer chains were confined to at least two different conformations or to different ordered states, since two resonance peaks are observed in the ^{13}C CP-MAS experiments for these two different methylene carbons, which represent the heterogeneity in the lyophilized sample. Also, the same crystalline arrangement for the polymer chains was obtained during the lyophilization of the PEI solution, taking into account that the XRPD patterns were identical for both samples. The signal at 42.9 ppm, which is still present after the lyophilization process, is associated with the crystalline peaks in the XRPD spectrum (Figure 1), being the signal at 44.5 ppm a contribution from amorphous segments that are undetectable in the XRPD experiments and only contribute to a higher background in the spectrum (Figure 1). It is important to mention that the heterogeneity presented for the lyophilized polymers cannot be observed directly from the XRPD profiles, as it was the case from the *ss*-NMR experiments (Figures 1 and 2).

In the ^{13}C CP-MAS experiments in the Cu complexes, the ^{13}C signal at 44.4 ppm remained, whereas the signal at 42.9 ppm was absent. These facts, together with the changes observed in the XRPD spectra, indicate that some rearrangement took place after the uptake of Cu and/or SO_4^{2-} ions. The absence of a second signal could have origin in the presence of copper, which induces the rapid relaxation of the nucleus in the proximity of the paramagnetic ion, precluding the observation of a second carbon signal.[48−51]

In addition, the ^{15}N CP-MAS spectra at natural abundance recorded for different samples of PEI were consistent with the observations of the corresponding ^{13}C spectra. Figure 2.II shows that the ^{15}N spectrum for lyophilized PEI 87 kDa presented two clearly differentiated resonances at −334.9 and −333.4 ppm. In the ^{15}N CP-MAS experiments, the distinctive chemical shifts for nitrogen are representative of the crystalline (−334.9 ppm) and amorphous domains (−333.4 ppm) as the ^{13}C resonance signals. For the Cu complexes, the ^{15}N signal was shifted to low frequencies after the coordination with Cu and/or SO_4^{2-} ions (−342.6 ppm, Figure 2), whereas the ^{13}C signal was shifted to high frequencies (44.5 ppm, Figure 2) as compared with the signal at 42.9 ppm in the crystallized sample. The ^{15}N CP-MAS experiments allowed determining that in the Cu(II) complexes the disposition and/or the chemical composition of the polymeric chains changed due to the presence of SO_4^{2-}, because the resonance signal from ^{15}N differs like in the nondoped polymers (lyophilized or crystallized). It is thus decisive to show that the molecular conformation in the Cu(II) complex is different from that observed in the crystallized and lyophilized samples. The behavior observed in the PEI 87 kDa samples was the same as that observed in the PEI 22 and 217 kDa samples.

Besides the fact that the coordinated nitrogens coordinated with Cu and the surrounding of the methylene carbon next to the paramagnetic ion may not be observed in the ^{15}N and ^{13}C CP-MAS experiments because the relaxation behavior is enhanced by the presence of the paramagnetic ions,[48−51] the ^{13}C and ^{15}N signals observed after the uptake of Cu might be associated with some changes in the molecular conformation or chemical environment of the polymeric segments

Considering mononuclear square-planar geometries for the Cu centers, four nitrogens are coordinated with Cu ions, and together with the XPS results where the ratio of N:Cu is ∼16:1 (Table 1), the ^{15}N signal observed in the CP-MAS experiments arises from 70% of the total nitrogen. The rest of the nitrogen nuclei (30%) did not contribute to the NMR signal due to the presence of the Cu enhancement relaxation. However, when the Cu ions were completely desorbed from the Cu(II)−PEI complex the ^{13}C and ^{15}N CP-MAS spectra remained identical, indicating that the Cu ions did not affect substantially the chemical structure or the order of the system in terms of crystallinity. In fact, the ones responsible for the crystalline domains were the sulfate ions in comparison with the incorporation of Cu to the polymer network, as observed through the XRPD results when the Cu complexes were prepared with $CuSO_4$ solution. In addition, the sulfate ions structurally retained in the polymer chains of PEI can be cooperating with the nitrogen atoms for the uptake of Cu and for that reason the amount of nitrogen involved in the coordination of Cu can be lower than 30%, explaining a not significant shift in the N 1s spectrum after the incorporation of

DOI: 10.1021/ma5023082
Macromolecules 2015, 48, 1115−1125

Table 2. T_1^H and T_2^H Relaxation Time Values in PEI Samples[a]

	T_1^H (ms)			
material	lyophilized	crystallized	Cu(II) complex	Cu(II)-desorbed
PEI 22 kDa	32	87	6.0	828
PEI 87 kDa	98	187	2.6	766
PEI 217 kDa	189	368	3.2	793
	T_2^H (ms)			
material	lyophilized	crystallized	Cu(II) complex	Cu(II)-desorbed
PEI 22 kDa	0.09 (40%), 0.52 (60%)	0.04 (65%), 0.33 (35%)	0.04	0.06 (90%), 0.24 (10%)
PEI 87 kDa	0.12 (56%), 0.44 (45%)	0.03 (80%), 0.19 (20%)	0.05	0.06 (93%), 0.77 (7%)
PEI 217 kDa	0.08 (56%), 0.35 (44%)	0.02 (60%), 0.26 (40%)	0.04	0.05 (90%), 1.06 (10%)

[a]The relative errors are within 3%.

Cu as in other Cu(II) complexes (Figure S3, Supporting Information).[36]

3.4. Measurements of ^{1}H Relaxation Times. As mentioned above, the *ss*-NMR results suggest the presence of heterogeneity in the samples studied, being more significant in the lyophilized sample than in the crystallized or Cu(II)−PEI samples. NMR relaxation times are valuable experimental parameters to test heterogeneity in solid samples. Different proton relaxation times were measured: ^{1}H longitudinal relaxation time (T_1^H), ^{1}H longitudinal relaxation time in the rotating frame ($T_1\rho^H$) and ^{1}H transverse relaxation time (T_2^H). The results are summarized in Table 2 and Table S2 in the Supporting Information.

The T_1^H relaxation times showed a single exponential decay for all the samples. At the time scale of this relaxation time, spin diffusion is effective enough to average out the contributions to T_1^H from different regions in the sample. By observing the results for the different samples, we found higher T_1^H for the crystallized samples than for the lyophilized ones, since in the crystallized polymers higher ordered structures with reduced mobility polymer chains are expected. In addition, higher T_1^H values were observed as the molecular weight of the polymer increased. With the coordination of Cu ions, the relaxation of protons in the Cu(II)−PEI samples was dramatically reduced due to the presence of the paramagnetic ions dispersed in the polymeric structure; however, the desorption of Cu produced an important increase in the T_1^H values (Table 2).[48,49]

The T_2^H decay for both the crystallized and lyophilized samples presented a double-exponential behavior with a short and long decay attributed to the hard and soft segments in the polymer material, respectively, since the faster decay is associated with crystalline regions. In addition, the estimated fraction of the crystalline phase was higher in the crystallized samples than in the lyophilized ones in all the cases. For the Cu(II) complexes, an important decrease in the T_2^H values was observed for all the complexes. The T_2^H decay presented a single-exponential behavior, as a consequence of the cross-link of the different polymer chains that coordinate the Cu and SO_4^{2-} ions. In this sense, the presence of Cu and SO_4^{2-} in 3.6% and 45% respectively was responsible for the homogeneous character of the polymeric segments in terms of mobility. After desorption of Cu, the T_2^H decay shows a double-exponential behavior with a slow decay component of about 10% and the faster decay still present in a significant proportion (~90%) (Figure 3 and Table 2). The appearance of a more mobile fraction might be associated with the release of Cu, which was retained in the polymer structure with the sulfate ions and/or amine groups, affecting the well-ordered domains of the Cu-

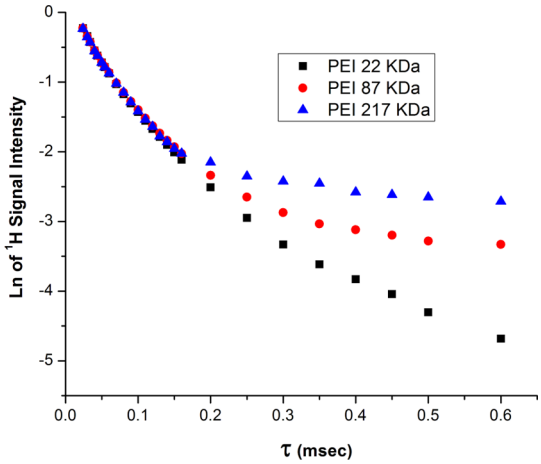

Figure 3. Semilog plot of the ^{1}H transverse magnetization decay in Cu(II)-desorbed samples of PEI.

complexes associated with sulfate ions. It is important to remark that the shortest T_2^H values were practically the same for all the Cu(II)-desorbed samples of PEI. Differences were observed for the longest T_2^H values where the mobility of the polymer chain is increased as the molecular weight increases (Figure 3 and Table 2).

The $T_1\rho^H$ values for the crystallized and lyophilized samples also show a double-exponential decay. The $T_1\rho^H$ values for the two decays are in the order of few hundreds of microseconds and some milliseconds (Table S2, Supporting Information). Because the $T_1\rho^H$ values are also affected by spin diffusion, the two components are only indicative of the presence of heterogeneity in the samples and were used as tentative values for setting up the ^{13}C CP-MAS discriminating experiments.

3.5. Edited ^{13}C CP-MAS Experiments. To assign the ^{13}C NMR signals in the *ss*-NMR experiments correctly and prove the heterogeneous character of the PEI samples directly, edited ^{13}C CP-MAS spectra were recorded. Figure 4 shows the delayed ^{13}C CP-MAS spectra of crystallized and lyophilized PEI 87 kDa with delayed times (τ_d) between 0 and 15 μs. It is clear that two well-resolved signals can be distinguished at 42.9 and 44.5 ppm in all the cases, even when the signal-to-noise ratio was affected.

As mentioned before, using the standard CP-MAS pulse sequence (τ_d = 0 μs), one single ^{13}C resonance was observed at 42.9 ppm for the crystallized sample. However, as the delay time increased, another signal can be observed at 44.5 ppm as a shoulder. As the delayed CP pulse sequence tests the strength of the ^{1}H−^{1}H dipolar interactions, the signal at 44.5 ppm can

DOI: 10.1021/ma5023082
Macromolecules 2015, 48, 1115−1125

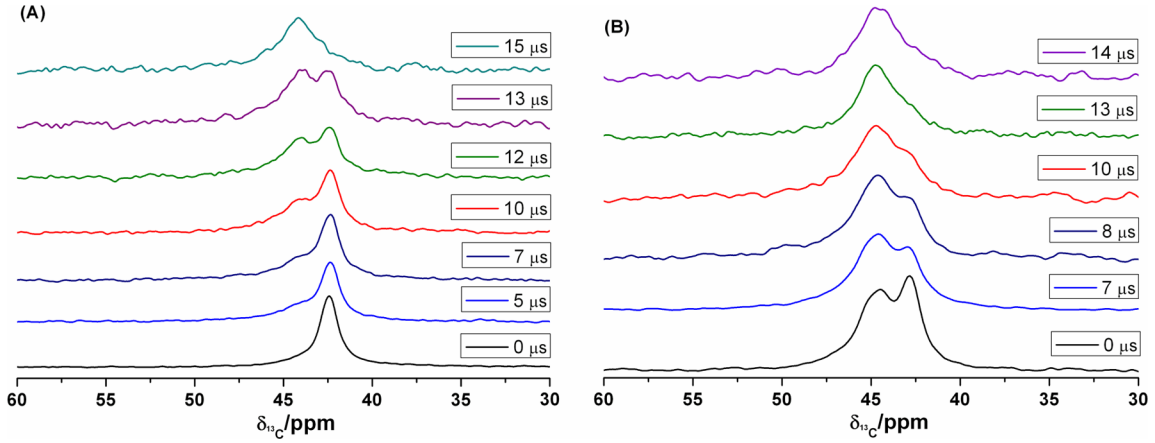

Figure 4. Delayed ^{13}C CP-MAS spectra for a crystallized sample of PEI 87 kDa (A) and a lyophilized sample of PEI 87 kDa (B) with different dynamic times τ_d as indicated (contact time: 200 μs).

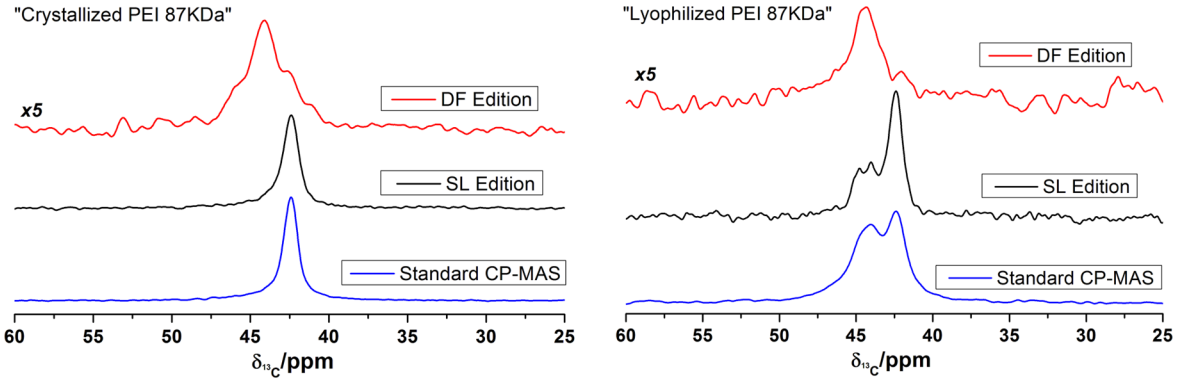

Figure 5. Edited ^{13}C CP-MAS techniques (DF and SL) and standard CP-MAS experiments in crystallized and lyophilized samples of PEI 87KDa, respectively.

be attributed to a mobile amorphous phase. At τ_d = 13 μs, the resonance signal at 44.5 ppm had the same intensity as the signal at lower chemical shift, and finally, at longer delay times (τ_d = 15 μs), the signal at 42.9 ppm was completely depleted (Figure 4A). The ^{13}C spectrum of the lyophilized sample presented two well-resolved resonances for a τ_d = 0 μs (Figure 4B). The spectrum can be modulated by increasing τ_d from 0 to 13 μs, when the lowest chemical shift signal was practically depleted and the only resonance signal that can be observed is at 44.5 ppm. Although the samples were obtained from different procedures, the dynamic behaviors of the components depicted by the ^{13}C resonances at 42.9 and 44.5 ppm were similar in both samples. A delayed CP was performed in the case of ^{15}N CP-MAS spectra, but the signal-to-noise ratio was dramatically affected and the resolved resonances could not be clearly observed.

The results obtained from the standard ^{13}C CP-MAS experiments showed that during the synthetic process, the PEI particles crystallized in the acidic medium, giving rise to apparent homogeneous samples (Figure 2). However, if a selective pulse sequence as delayed CP step was applied, an important degree of heterogeneity was observed (Figure 4A). In contrast, when the solid was dissolved and the solution was lyophilized, the polymeric chains can be confined to regions with different molecular mobility, determining "crystalline" or "amorphous" segments (Figure 4B). In addition, when any of the solid samples were dissolved, if any molecular heterogeneity exists, the polymer chains acquire an average molecular motion within the solvent, giving the isotropic chemical shift obtained for PEI 87 kDa in D_2O solution at 43.5 ppm (Figure 2A). To further investigate the origin of the two resonances observed in the ^{13}C spectra for different samples, edited ^{13}C CP-MAS NMR experiments by using ^{1}H dipolar filter (DF) and ^{1}H spin-lock filter (SL) were performed to select the magnetization coming from the amorphous or crystalline regions, respectively.

The ^{13}C DF/CP-MAS technique is more sensitive to mobile components at short contact times than the standard ^{13}C CP-MAS experiments, where the magnetization coming from rigid regions is enhanced against the magnetization from the amorphous mobile regions, due to the strong dipolar couplings between protons and carbons in crystalline regions. Making use of the fact that the $T_1\rho^H$ for the crystalline domains is much longer than that for the amorphous domains, at least at room temperature for polymers, the ^{13}C SL/CP-MAS experiment is effective to select ^{13}C magnetization coming from rigid domains.

Figure 5 displays the ^{13}C DF/CP-MAS and SL/CP-MAS spectra in comparison with the standard CP-MAS spectra obtained for the crystallized and lyophilized samples of PEI 87 kDa. In the case of the lyophilized sample, the ^{13}C SL/CP-MAS spectrum exhibits an important decrease in the intensity of the signal at 44.5 ppm relative to the signal at 42.9 ppm. In contrast, when ^{1}H-DF was used, the resonance signal at 42.9 ppm was dramatically affected, while the signal at 44.5 ppm was practically unaltered. These results confirm that resonance signals at 44.5 and 42.9 ppm arise from the magnetization of

DOI: 10.1021/ma5023082
Macromolecules 2015, 48, 1115−1125

different methylene environments ($-CH_2-$) present in the amorphous and crystalline regions, respectively.

For the crystallized PEI 87 kDa sample, the standard ^{13}C CP-MAS and SL/CP-MAS spectra show the same signal at 42.9 ppm, corresponding to the higher ordered phase. However, the ^{13}C DF/CP-MAS spectrum shows that the high frequency resonance comes from the noise with the corresponding vanishing contribution of the crystalline component. It is important to remark that the more mobile methylene carbons in the crystallized PEI samples are observed only if the ^{13}C CP-MAS spectra are acquired with a selective pulse sequence. In contrast, the more restricted methylene carbons with a constrained mobility are observed in all the ^{13}C CP-MAS spectra. The results described here for PEI 87 kDa were also observed with the samples with other molecular weights.

The DF and SL experiments were performed in the Cu(II)−PEI complexes. The results corresponding to the PEI 87 kDa-Cu complex are shown in Figure 6. The selective CP

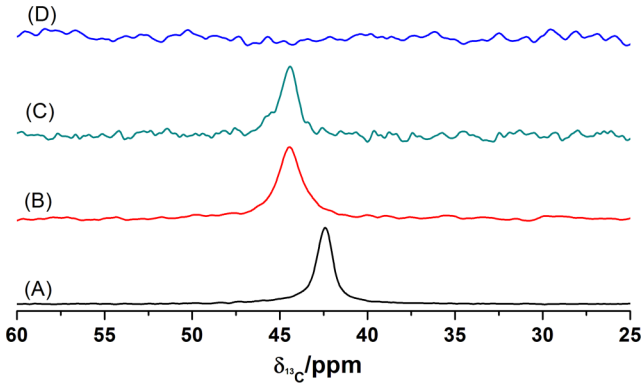

Figure 6. Standard ^{13}C CP-MAS in crystallized PEI 87 kDa (A) and in Cu(II)−PEI 87 kDa (B). SL− (C) and DF−^{13}C CP-MAS experiments (D) in Cu(II) complex samples of PEI 87 kDa.

experiments showed that Cu(II) complexes are homogeneous crystalline samples, as the ^{13}C SL/CP-MAS spectrum showed that a new crystalline domain was organized by the metal ion. In addition, the ^{13}C DF/CP-MAS spectrum showed no resonance signal, indicating the homogeneity of the Cu complexes. These results are significantly different from those obtained for the lyophilized and crystalline PEI samples (Figure 5). These results were confirmed with the delayed CP spectra of the Cu(II) complexes, which showed only one component for all the τ_d selected. However, this shift in the ^{13}C signal was not directly associated with a paramagnetic effect induced by Cu ions, since the ^{13}C SL/CP-MAS spectrum shows that a new crystalline domain was organized by the metal ion. The absence of signal in the ^{13}C DF/CP-MAS is consistent with the high ordered and homogeneous behavior of the Cu(II) complexes. In addition, the τ_d edited ^{13}C CP-MAS spectra of the Cu(II) complexes showed only one component, supporting that the Cu complexes are in a well-ordered state. To corroborate this affirmation, the Cu(II)-desorbed samples were analyzed by the same edited ^{13}C experiments (Figure S6, Supporting Information). Here again, the same results were obtained, demonstrating not only the well and ordered state of the polymeric segments in the Cu(II)-desorbed samples but also that the Cu(II)-complexes are ordered and that the relaxation effect of the paramagnetic ions did not affect the visualization of other signals in the ^{13}C CP-MAS experiments (Figure 6 and Figure S6, Supporting Information). However, in the Cu(II)-desorbed PEI samples, 7% of amorphous regions in PEI 87 kDa and 10% in PEI 22 and 217 kDa were observed in the T_2^H experiments (Table 2), but these could not be observed in the ^{13}C CP-MAS experiments or even in the edited or ^{13}C direct polarization experiments.

3.6. ^{13}C Direct Polarization Experiments. With the crystalline and amorphous regions identified through the edited ^{13}C NMR experiments, ^{13}C direct polarization experiments were performed for the quantification of each fraction in the different samples of PEI 87 kDa and the results are shown in

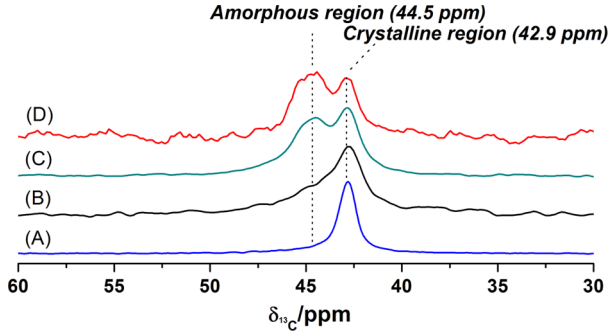

Figure 7. ^{13}C MAS spectra for crystallized PEI 87 kDa sample with $^{13}C\{^1H\}$ cross-polarization (A) or with ^{13}C direct polarization (B) and for lyophilized PEI 87 kDa sample with $^{13}C\{^1H\}$ cross-polarization (C) or with ^{13}C direct polarization (D).

Figure 7. The results of the fitting performed in the quantitative ^{13}C MAS NMR spectra for all the samples are summarized in Table 3 and in Figures S7 and S8 in the Supporting

Table 3. Crystallinity Degree in PEI Samples Determined by the Quantitative ^{13}C MAS Experiments

	crystallinity degree	
material	lyophilized	crystallized
PEI 22 kDa	13	88
PEI 87 kDa	31	60
PEI 217 kDa	30	38

Information. For the calculations of the percentage of the crystalline and amorphous regions, the chemical shifts at 42.9 and 44.5 ppm were used in the crystallized and lyophilized PEI samples, respectively. The crystallinity of the crystallized samples was higher than that of the lyophilized ones. The amorphous components increased as the molecular weights of PEI in the crystallized samples increased. In the case of the Cu(II)−PEI complexes and the Cu(II)-desorbed PEI samples, the correct determination of the crystallinity was not possible from the ^{13}C direct polarization experiments since only one NMR signal was observed.

3.7. 2D *ss*-NMR Experiments. Taking into account the simple chemical structure of the monomeric unit of the PEI samples, we performed 2D $^1H-^{13}C$ WISE experiments to obtain the average $^1H-^1H$ dipolar coupling associated with the carbon nucleus present in each phase. Then, the average line-width of the ^1H resonance line projections associated with each ^{13}C is a measure of the $^1H-^1H$ dipolar interactions. Figure 8 displays the 2D $^1H-^{13}C$ WISE spectra for the PEI 87 kDa samples together with their Cu complexes, and Table 4

DOI: 10.1021/ma5023082
Macromolecules 2015, 48, 1115−1125

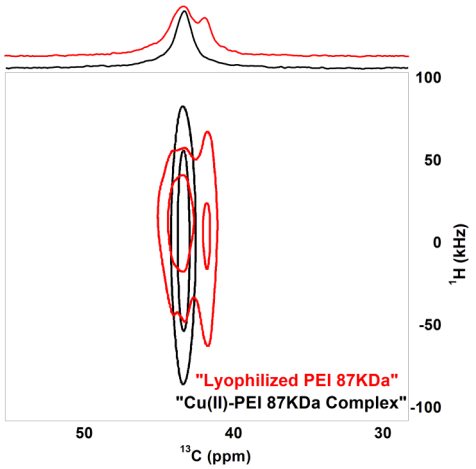

Figure 8. 2D WISE spectra for lyophilized and Cu(II) complex of PEI 87 kDa.

Table 4. Full Width at Half Height (fwhh) Values for the ^{1}H Projection Corresponding to the ^{13}C Resonance Signals for the Indicated PEI Samples in the 2D WISE Experiments[a]

	2D WISE fwhh (kHz)			
material	lyophilized (44.5/42.9 ppm)	crystallized (42.9 ppm)	Cu(II) complex (44.5 ppm)	Cu(II)-desorbed (44.4 ppm)
PEI 22 kDa	55/68	74	72	75
PEI 87 kDa	43/71	80	75	77
PEI 217 kDa	40/70	78	73	75

[a]The uncertainty in all fwhh values reported for the ^{1}H projection is less than ±2 kHz.

summarizes the full width at half height (fwhh) of the ^{1}H projections. It is clearly observed that the lyophilized PEI sample was not homogeneous. There, the smaller fwhh value (higher mobility region) corresponds to the carbon signal at 44.5 ppm, whereas the higher fwhh value (less mobile or rigid region) corresponds to the carbon resonance at 42.9 ppm. When the Cu ions were introduced in the polymeric structure, a homogeneous character was observed since only one component was present in the sample, in agreement with the previous results given by the edited ^{13}C spectra. In the Cu complexes, the line-width of the ^{1}H projection corresponding to the ^{13}C signal at 44.5 ppm showed a significant increase in comparison with that corresponding to the same carbon signal in the lyophilized sample (Table 4 and Figure 8). This observation indicates that mobility was reduced with the coordination of SO_4^{2-} ions, since when the Cu ions were desorbed, the same fwhh values were obtained (Table 4), in concordance with all the previous results presented here. In all the cases, the fwhh values for the crystallized samples, including the Cu(II) complexes and Cu(II)-desorbed samples, were the highest ones. It is important to remark that the results obtained for the Cu(II)−PEI and Cu(II)-desorbed samples clearly show that, in terms of chemical environment and/or molecular distribution of the polymer chain, the chemical shift at 44.4 ppm is not related to the signal at 44.5 ppm in the lyophilized samples (Figure 2 and Table 4).

The 2D ^{1}H−^{13}C HETCOR spectra allowed correlating the different ^{13}C nuclei with the protons that were directly linked or nearby. The results for PEI 87 kDa are shown in Figure 9. It can be clearly seen that each type of carbon correlates with similar qualities of protons but different from each other. In both samples of PEI, the methylene carbons (45−42 ppm) correlated with their directly bounded protons (~3 ppm) as well as with the nonbounded protons of the amino groups (~9 ppm). In general, the "more rigid" segments, which correlated with the 42.9 ppm carbon signal, presented higher ^{1}H chemical shifts (δ_{1H}) than the "more mobile" components, which correlated with the 44.5 ppm carbon signal. This indicates that the polymer chains in the different phases of PEI 87 kDa were in different physical environments that are associated with regions with a high degree of order (crystalline) or disorder (amorphous), in concordance with the information obtained from the edited ^{13}C CP-MAS spectra and XRPD experiments. For the Cu complexes, the signals observed may arise from the noncoordinated segments since Cu ions induce an strong source of relaxation affecting the resonance signal in the proximmity of the sphere of Cu(II) centers.[49] However, the changes in the 2D-spectrum with PEI and Cu ions were similar to those observed in the lyophillized samples related to the signal at 44.5 ppm, and the environment and disposition of the polymer chains were different considering the information obtained in the ^{15}N CP-MAS spectra. In addition, the homogeneous character in terms of regularity of the disposition of the polymeric segments can be inferred from the spectra of the Cu complexes and crystallized samples of PEI since the ^{13}C correlated with two qualities of protons (−CH_2− and −NH−). In the lyophilized samples, the heterogeneous character can be clearly observed at both ^{1}H and ^{13}C dimensions. Finally, for the Cu(II)-desorbed polymers, the same results were the same as for the Cu(II)−PEI complexes (Figure S11, Supporting Information), indicating that the ones responsible for the disposition and similarity in the chemical environment were the SO_4^{2-} ions, as proved with the edited ^{13}C CP-MAS, direct polarization ^{13}C, 2D *ss*-NMR and T_2^H experiments performed in the different samples studied in this work.

In general, the observations corresponding to the 2D experiments performed in the PEI 22 kDa and 217 kDa samples are coincident with the behavior observed for PEI 87 kDa.

4. CONCLUSIONS

In this work, we proved that *ss*-NMR is a valuable tool to study the dynamics and homogeneity in crystallized or lyophilized samples of linear poly(ethylenimine hydrochloride) (PEI·HCl) polymers. Although the results of XRPD showed no significant differences between different samples, *ss*-NMR through edited ^{13}C CP-MAS spectra (τ_d times, DF/and SL/^{13}C-MAS) allowed demonstrating the heterogeneity in crystallized and lyophilized samples of PEI, as well as ^{15}N CP-MAS spectra, associated with the presence of crystalline and amorphous domains. In addition, the results of 2D ^{1}H−^{13}C WISE and HETCOR experiments showed coexisting polymeric regions with different chemical environments, being the carbon signal at 44.5 ppm the more mobile region and the signal at 42.9 ppm the less mobile region, consistent with the T_2^H times. The lyophilization of the different solutions of PEI caused an increase in the amorphous components even when some ordered domains were present in a lower extent as was demonstrated with the ^{13}C direct polarization experiments.

The coordination of Cu and SO_4^{2-} ions involved polymeric regions with different molecular dynamics in the PEI samples, producing a significant reduction in the molecular mobility of the polymer chains of PEI and being more homogeneous than

DOI: 10.1021/ma5023082
Macromolecules 2015, 48, 1115−1125

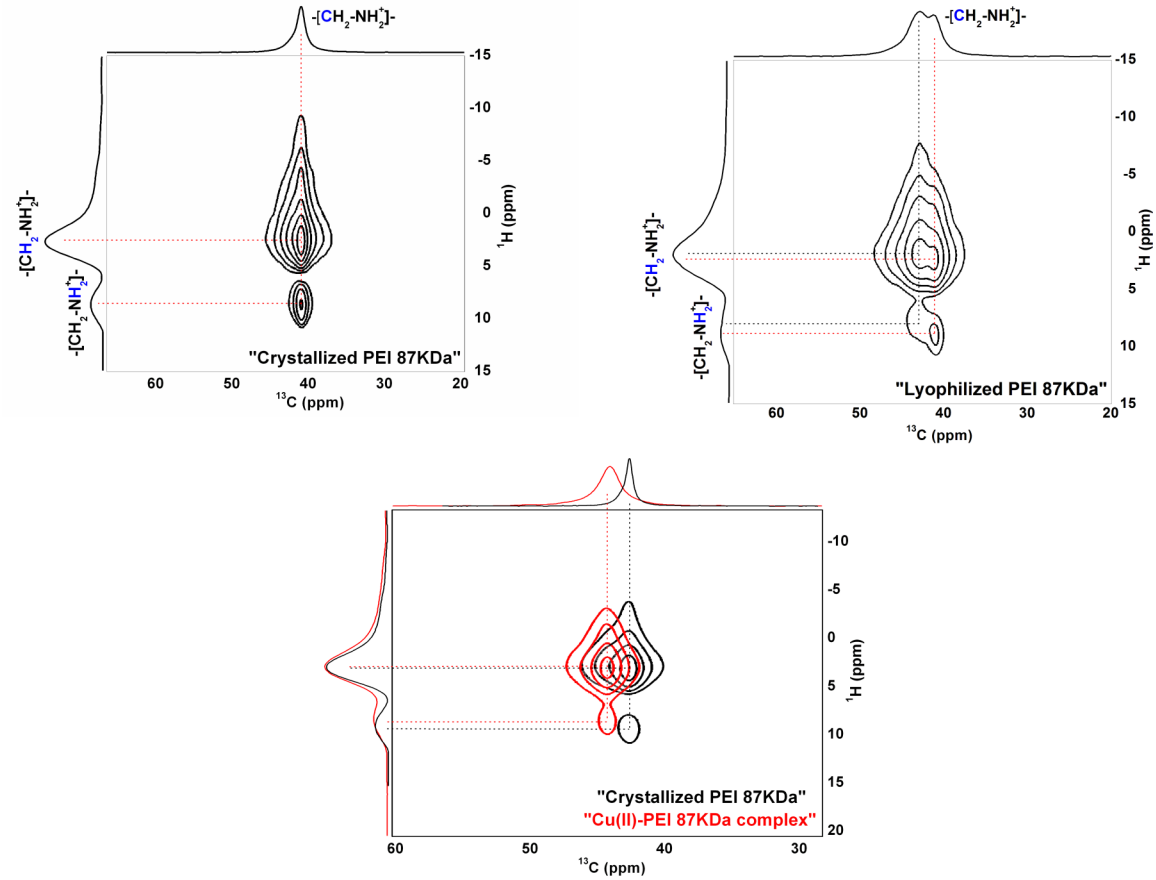

Figure 9. 2D $^{1}H-^{13}C$ HETCOR spectra for crystallized, lyophilized and superimposed crystallized/Cu(II)-complex of samples of PEI 87 kDa.

the crystallized or lyophilized samples, regardless of the molecular weights. The measurements of T_2^H showed that the rigid component was quantitative. It is important to remark that the rigidity of the entire polymer network was produced with 3−4 wt % of Cu and 40−52 wt % of SO_4^{2-} according with the XPS, XRF, and elemental analysis results in the different Cu(II)−PEI complexes. The complete desorption of Cu from the Cu(II)−PEI polymers demonstrates that the SO_4^{2-} ions were responsible for the high order and homogeneous character in both Cu(II)−PEI and Cu(II)-desorbed samples, as observed from the T_2^H, edited *ss*-NMR and 2D *ss*-NMR experiments.

The other PEI samples (22 and 217 kDa) showed the same behavior as PEI 87 kDa, indicating that lyophilized and crystallized samples display similar XRPD patterns, however, the heterogeneous character in terms of local mobility can only be obtained and quantified from the *ss*-NMR studies reported here.

■ ASSOCIATED CONTENT

Supporting Information

Loading capacities of Cu and S, XPS spectra, $T_1\rho^H$ values, XPS spectra, expanded 2D *ss*-NMR spectra, and additional 1D/2D *ss*-NMR results of PEI, Cu(II)−PEI, and Cu(II)-desorbed materials. This material is available free of charge via the Internet at http://pubs.acs.org.

■ AUTHOR INFORMATION

Corresponding Author

*(J.M.L.-M.) Telephone/fax: +54-11-49648200, int. 8351. E-mail: lazarojm@ffyb.uba.ar).

Notes

The authors declare no competing financial interest.

■ ACKNOWLEDGMENTS

We express thanks for the financial support from ANPCYT (PICT 2010-1096, PICT 2012-0151 & 0716), Universidad de Buenos Aires (UBACyT 2013-2016/021BA & 043BA), CONICET (PIP 2014-2016/130 & 746), and SeCyT Universidad Nacional de Córdoba.

■ REFERENCES

(1) Herlem, G.; Lakard, B. *J. Chem. Phys.* **2004**, *120*, 9376−9382.
(2) Halacheva, S.; Price, G. J.; Garamus, V. M. *Macromolecules* **2011**, *44*, 7394−7404.
(3) Holycross, D. R.; Chai, M. *Macromolecules* **2013**, *46*, 6891−6897.
(4) Lambermont-Thijs, H. M. L.; Van Der Woerdt, F. S.; Baumgaertel, A.; Bonami, L.; Du Prez, F. E.; Schubert, U. S.; Hoogenboom, R. *Macromolecules* **2010**, *43*, 927−933.
(5) Glatzhofer, D.; Erickson, M.; Frech, R.; Yepez, F.; Furneaux, J. *Solid State Ionics* **2005**, *176*, 2861−2865.
(6) Harris, C. S.; Ratner, M. A.; Shriver, D. F. *Macromolecules* **1987**, *20*, 1778−1781.
(7) Doyle, R. P.; Chen, X.; Macrae, M.; Srungavarapu, A.; Smith, L. J.; Gopinadhan, M.; Osuji, C. O.; Granados-focil, S. *Macromolecules* **2014**, *47*, 3401−3408.
(8) Spoden, G. a; Besold, K.; Krauter, S.; Plachter, B.; Hanik, N.; Kilbinger, A. F. M.; Lambert, C.; Florin, L. *Antimicrob. Agents Chemother.* **2012**, *56*, 75−82.
(9) Jäger, M.; Schubert, S.; Ochrimenko, S.; Fischer, D.; Schubert, U. S. *Chem. Soc. Rev.* **2012**, *41*, 4755−4767.
(10) Lakshmipraba, J.; Arunachalam, S.; Avinash, D. *Eur. J. Med. Chem.* **2011**, *46*, 3013−3021.

DOI: 10.1021/ma5023082
Macromolecules 2015, 48, 1115−1125

(11) Choudhury, C. K.; Kumar, A.; Roy, S. *Biomacromolecules* **2013**, *14*, 3759−3768.
(12) Fukumoto, Y.; Obata, Y.; Ishibashi, K.; Tamura, N. *Cytotechnology* **2010**, *62*, 73−82.
(13) Guo, Q.; Shi, S.; Wang, X.; Kan, B.; Gu, Y.; Shi, X.; Luo, F.; Zhao, X.; Wei, Y.; Qian, Z. *Int. J. Pharm.* **2009**, *379*, 82−89.
(14) Brissault, B.; Kichler, A.; Guis, C.; Leborgne, C.; Danos, O. *Bioconjugate Chem.* **2003**, *14*, 581−587.
(15) Nguyen, H.; Lemieux, P.; Vinogradov, S. V.; Gebhart, C. L.; Gue, N. *Gene Ther.* **2000**, *7*, 126−138.
(16) Englert, C.; Tauhardt, L.; Hartlieb, M.; Kempe, K.; Gottschaldt, M.; Schubert, U. S. *Biomacromolecules* **2014**, *15*, 1124−1131.
(17) Ziebarth, J. D.; Wang, Y. *Biomacromolecules* **2011**, *11*, 1−29.
(18) Eliyahu, H.; Barenholz, Y.; Domb, a J. *Molecules* **2005**, *10*, 34−64.
(19) Chatani, Y.; Tadokoro, H.; Saegusa, T.; Ikeda, H. *Macromolecules* **1981**, *14*, 315−321.
(20) Chatani, Y.; Kobatake, T.; Tadokoro, H.; Tanaka, R. *Macromolecules* **1982**, *15*, 170−176.
(21) Kakuda, H.; Okada, T.; Otsuka, M.; Katsumoto, Y.; Hasegawa, T. *Anal. Bioanal. Chem.* **2009**, *393*, 367−376.
(22) Shi, H.; Zhao, Y.; Zhang, X.; Jiang, S.; Wang, D.; Han, C. C.; Xu, D. *Macromolecules* **2004**, *37*, 9933−9940.
(23) Hashida, T.; Tashiro, K.; Aoshima, S.; Inaki, Y. *Macromolecules* **2002**, *35*, 4330−4336.
(24) Kakuda, H.; Okada, T.; Hasegawa, T. *J. Phys. Chem. B* **2008**, *112*, 12940−12945.
(25) Hashida, T.; Tashiro, K.; Ito, K.; Takata, M.; Sasaki, S.; Masunaga, H. *Macromolecules* **2010**, *43*, 402−408.
(26) Kakuda, H.; Okada, T.; Hasegawa, T. *J. Phys. Chem. B* **2009**, *113*, 13910−13916.
(27) Koper, G. J. M.; Van Duijvenbode, R. C.; Stam, D. D. P. W.; Steuerle, U.; Borkovec, M. *Macromolecules* **2003**, *36*, 2500−2507.
(28) Shi, H.; Zhao, Y.; Jiang, S.; Rottstegge, J.; Xin, J. H.; Wang, D.; Xu, D. *Macromolecules* **2007**, *40*, 3198−3203.
(29) Zappia, M. P.; Bernabo, G.; Billi, S. C.; Frasch, A. C.; Ceriani, M. F.; Brocco, M. A. *BMC Neurosci.* **2012**, *13*, 78.
(30) Yadava, P.; Gibbs, M.; Castro, C.; Hughes, J. a. *AAPS PharmSciTech* **2008**, *9*, 335−341.
(31) Andersen, M. Ø.; Howard, K. a; Paludan, S. R.; Besenbacher, F.; Kjems, J. *Biomaterials* **2008**, *29*, 506−512.
(32) Sui, D.; Fan, H.; Li, J.; Li, Y.; Li, Q.; Sun, T. *Talanta* **2013**, *114*, 276−282.
(33) Tang, Y.; Ma, Q.; Luo, Y.; Zhai, L.; Che, Y.; Meng, F. *J. Appl. Polym. Sci.* **2013**, *9*, 1799−1805.
(34) Zelewsky, A. Von; Barbosa, L.; Schlzipfer, C. W. *Coord. Chem. Rev.* **1993**, *123*, 229−246.
(35) Kobayashi, S.; Hiroishi, K.; Tokunoh, M.; Saegusai, T. *Macromolecules* **1987**, *20*, 1496−1500.
(36) Lázaro Martínez, J. M.; Rodríguez-Castellón, E.; Sánchez, R. M. T.; Denaday, L. R.; Buldain, G. Y.; Campo Dall' Orto, V. *J. Mol. Catal., Part A: Chem.* **2011**, *339*, 43−51.
(37) Lázaro Martínez, J. M.; Leal Denis, M. F.; Piehl, L. L.; de Celis, E. R.; Buldain, G. Y.; Campo Dall' Orto, V. *Appl. Catal., Part B: Environ.* **2008**, *82*, 273−283.
(38) Lombardo Lupano, L. V.; Lázaro Martínez, J. M.; Piehl, L. L.; Rubín de Celis, E.; Torres Sánchez, R. M.; Campo Dall' Orto, V. *Langmuir* **2014**, *30*, 2903−2913.
(39) Poulston, S.; Parlett, P. M.; Stone, P. *Surf. Interface Anal.* **1996**, *24*, 811−820.
(40) Fung, B. M.; Khitrin, A. K.; Ermolaev, K. *J. Magn. Reson.* **2000**, *101*, 97−101.
(41) Hu, W.; Schmidt-Rohr, K. *Polymer* **2000**, *41*, 2979−2987.
(42) Asano, A.; Tanaka, C.; Murata, Y. *Polymer* **2007**, *48*, 3809−3816.
(43) Jenkins, J. E.; Seitz, M. E.; Buitrago, C. F.; Winey, K. I.; Opper, K. L.; Baughman, T. W.; Wagener, K. B.; Alam, T. M. *Polymer* **2012**, *53*, 3917−3927.
(44) Schmidt-Rohr, K.; Clauss, J.; Spiess, H. W. *Macromolecules* **1992**, *25*, 3273−3277.
(45) Van Rossum, B. J.; Förster, H.; de Groot, H. J. M. *J. Magn. Reson.* **1997**, *124*, 516−519.
(46) Avgouropoulos, G.; Ioannides, T. *Appl. Catal. Part A: Gen.* **2003**, *244*, 155−167.
(47) Yuan, J. J.; Jin, R. H. *Langmuir* **2005**, *21*, 3136−3145.
(48) Aguiar, P. M.; Katz, M. J.; Leznoff, D. B.; Kroeker, S. *Phys. Chem. Chem. Phys.* **2009**, *11*, 6925−6934.
(49) Bertini, I.; Luchinat, C.; Parigi, G.; Pierattelli, R. *Dalt. Trans.* **2008**, 3782−3790.
(50) Lázaro-Martínez, J. M.; Monti, G. A.; Chattah, A. K. *Polymer* **2013**, *54*, 5214−5221.
(51) Lázaro Martínez, J. M.; Chattah, A. K.; Monti, G. A.; Leal Denis, M. F.; Buldain, G. Y.; Campo Dall' Orto, V. *Polymer* **2008**, *49*, 5482−5489.

DOI: 10.1021/ma5023082
Macromolecules 2015, 48, 1115−1125